



Published in final edited form as:

J Org Chem. 2007 March 30; 72(7): 2469–2475. doi:10.1021/jo062526t.

Enthalpy (ΔH) and Entropy (ΔS) for π -Stacking Interactions in near-Sandwich Configurations: The Relative Importance of Electrostatic, Dispersive, and Charge-Transfer Effects

Benjamin W. Gung, Xiaowen Xue, and Yan Zou

Department of Chemistry & Biochemistry, Miami University, Oxford, OH 45056,
gungbw@muohio.edu

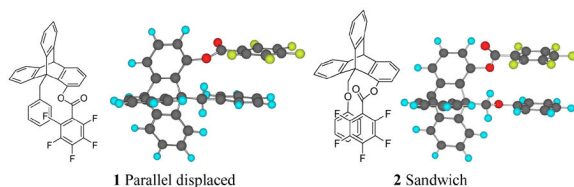
Abstract

Interactions between two aromatic rings with various substituents in a near-sandwich configuration have been quantitatively studied using the triptycene derived molecular models. This model system allows a stacking arrangement of two arenes to assume a near perfect face-to-face configuration in its ground state conformation. Comparing to our previous study of the parallel displaced configuration, repulsive interactions are predominant for most arenes currently studied. However, if one arene is strongly electron-deficient (Ar_2 = pentafluorobenzoate), attractive interactions were observed regardless of the character of the other arene (Ar_1). For stacking interactions between $Me_2NC_6H_4$ and C_6F_5CO groups, a ΔH of -1.84 ± 0.2 kcal/mol and a ΔS of -2.9 ± 0.8 cal/mol·K were determined. The general trend in the attractive stacking interaction towards a pentafluorobenzoate is $Me_2NC_6H_4 > Me_3C_6H_2 > Me_2C_6H_3 > MeC_6H_4 > MeOC_6H_4 > C_6H_5 > O_2NC_6H_4$. The observed trend is consistent with a donor-acceptor relationship and the acceptor is a C_6F_5CO group.

Introduction

Aromatic interactions play important roles in biological recognition and crystal engineering.^{1,2} Widespread interest have been shown in the development of models to improve our understanding of these interactions.^{3–5} The two most noted models with strategies to quantify aromatic interactions in the stacking conformation include the 1,8-diarylnaphthalene system by Cozzi, Siegel, and co-workers and the double mutant cycle system by Hunter and coworkers.^{6–9} However, each model system has its limitations and the previous models were either too restrictive or too flexible.^{8–11} There has not been enough quantitative studies to compare and reach a generally-agreed value for the magnitude of aromatic interactions in solution.⁵ Other studies involving the edge-to-face conformation have been reported.^{12–14} This study is focused on the face-to-face or sandwich configuration.

Recently we reported our studies on aromatic interactions using the triptycene derived model system,^{15,16} which allows the arenes to interact near their van der Waals' contact and quantitative determination of the magnitude of interaction was achieved. Our previous study involved arene-arene interactions in the parallel displaced configurations (**1**), i.e., the two arenes are parallel to each other with the center of one arene on top of the edge of the other. Through molecular modeling, we have found that by a small modification to the previous model compound, the arenes can be arranged to assume a near-sandwich configuration in the *syn* rotamer of **2**.



Currently little experimental data are available on the magnitude of arene interactions in solution. Although the significant role played by quadrupole moments of benzene and hexafluorobenzene has been elegantly presented,^{17–20} it seems that no agreement has been reached on whether electrostatic interactions alone control aromatic interactions.⁵ The consideration of quadrupole moments provides a simple way to visualize the charge distribution of aromatics and correctly predicts the preferred geometry of symmetrically substituted arene interactions. However, if the arenes are stacked at van der Waals distance, it would not be appropriate for the interactions to be quantitatively modeled as just a quadrupole-quadrupole interaction.^{20,21} In fact, recent high level theoretical studies have indicated that electrostatic forces alone cannot rationalize the energetic ordering of substituent effects.²² In general, theoretical studies have demonstrated the importance of dispersive forces.⁵ Our study has shown that in addition to electrostatic and dispersive forces, charge transfer or donor-acceptor interactions also play a role in aromatic interactions.¹⁶ We have recently reported the observation that a charge-transfer band was observed in the stacking interactions between a *N,N*-dimethylaminophenyl group and a pentafluorobenzoate group in a parallel-displaced configuration.¹⁶ This study shows that charge transfer interactions are also present for the same arene pair in a near sandwich configuration. Our data are consistent with the view that electrostatic, dispersive, and donor-acceptor forces all play a role in aromatic interactions in organic solvents. The relative importance of each force depends on the characteristics of the two arenes involved.

Results

As a result of molecular modeling studies, a modification to our recently reported model compounds was made in order to study aromatic interactions in the sandwich configuration. This calls for an insertion of an oxygen atom into our previous model between the bridgehead (C9) CH₂ group and the phenyl group. The compounds used in this study and their syntheses are summarized in Scheme 1. We will briefly describe the synthetic procedures.

Synthesis of the model compounds

The preparation of the desired compounds **6a–12i** started with a Diels-Alder reaction. Various anthraceny ethers **3** were prepared according to literature procedures^{23,24} and were allowed to react with the dienophile *p*-benzoquinone. The Diels-Alder reaction was followed by an equilibration/aromatization with KOAc to produce the triptycene derivative **4**. The less sterically hindered phenolic OH group at C4 was protected by a pivaloyl group to produce ester **5**. The pivaloyl group was chosen to be the spectator group to increase the solubility of these model compounds. The synthesis was completed with acylation reaction with substituted benzoyl chloride Ar₂COCl to afford the desired model compounds **6a–12i**.

Conformations of the *syn* and *anti* isomers

The two arenes are denoted as Ar₁ and Ar₂ with Ar₁ attached to the bridgehead carbon (C9) and Ar₂ attached to C1 of the triptycene system. Ar₁ and Ar₂ are face-to-face and within van der Waals' contact distance in the *syn* conformation. In the *anti* conformation, the Ar₁ group bisects the triptycene skeleton and the Ar₂ group assumes the perpendicular arrangement from the triptycene skeleton. It appears to be an edge-to-face arrangement between Ar₁ and Ar₂ in

the anti conformation. However, the distance between the C-H of Ar₁ and the π-face of Ar₂ is not optimal and the substituent effects do not correlate with the potential edge-to-face interaction in the anti conformation. As shown in Scheme 1, the Ar₁ groups range from mono-substituted *para*-X-phenyl to multiple methyl or methoxy substituted phenyl groups. The substituent X is varied from a strongly electron-donating group such as NMe₂ to an electron-withdrawing group such as NO₂. The Ar₂ groups also involve both mono-substituted benzoate and an increasingly electron-deficient arene by the increase of fluorine atoms on the aromatic ring. Molecular modeling via MacroModel (version 7.0, force field: MMFFs) shows a stable near-sandwich configuration between Ar₁ and Ar₂ in model compound **7a** where Ar₂ = C₆F₅, Figure 1. It is important to point out that the structures shown here were modeled by molecular mechanics, therefore, the sandwich conformation is stable based on steric and electrostatic effects alone. Other electronic effects such as dispersion forces can only be estimated by using more sophisticated electronic models. The only apparent repulsive close contact in the *syn* conformation (a, Figure 1) is between the oxygen atom at C1 and the one at the bridgehead CH₂. The arenes are far enough from each other in the *anti* conformer (b, Figure 1), neither steric and nor stacking interactions are present. The only potential interaction between Ar₁ and Ar₂ in the anti conformation is the attractive edge-to-face interaction mentioned above. Therefore any preference for the *syn* conformation should be the results of attractive interactions from the stacking orientation rather than repulsions from the anti conformer.

Variable Temperature NMR Spectroscopy

A variable temperature NMR study was carried out using these model compounds. Two conformational isomers, the *syn* and the *anti*, can be observed at low temperatures. This is due to the slow rotation of the bridgehead CH₂ group in these compounds on the NMR time scale, which allows the integration and the determination of the *syn/anti* isomer ratio for each compound (Figure 2). It is important to point out that the conformational freedom is rather limited for either the *anti* or the *syn* isomers. The C1 ester linkage prefers the *s-trans* conformation (Figure 1) by ~4.5 kcal/mol to the alternative *s-cis* conformation to avoid oxygen lone pair repulsion.^{25,26} Furthermore, the Ar₂C(=O)-O bond prefers to be nearly perpendicular to the triptycene arene plane which allows a parallel alignment between Ar₁ and Ar₂, Figure 1. Thus the *syn/anti* ratio is effectively the equilibrium constant between the stacked (or *syn*) and the separated (or *anti*) arene conformations. Since statistically two *syn* and one *anti* conformer are expected, the equilibrium constant, K_{eq}, should be 1/2·*syn/anti* ratio. The Ar₁OCH₂ protons are diastereotopic in the *syn* conformational isomer and display an *AB* quartet while they are enantiomeric in the *anti* conformation and appear as a singlet. The experimentally determined *syn/anti* ratios in CDCl₃ at different temperatures are shown in Table 1.

The ratio changes significantly with temperature when a model compound displays a large *syn/anti* ratio. This enables us to obtain both ΔH and ΔS by using the van't Hoff equation (1). Considering the importance of entropic effects in noncovalent interactions,¹¹ this study provides information for π- stacking that has not been reported from previous systems. Thermodynamic parameters are collected in Tables 2–4. Some caution should be taken with these data since the enthalpy and entropy obtained using the van't Hoff equation assume a constant enthalpy value in the surveyed temperature range which may or may not be true.

$$\ln K_{eq} = -\Delta H^\circ / RT + \Delta S^\circ / R \quad (K_{eq} = 1/2 \cdot \text{syn/anti}, R = \text{gas constant}) \quad (1)$$

Discussion

As shown in Table 1, the largest *syn/anti* ratio was obtained for compound **6a**, where $\text{Ar}_1 = \text{C}_6\text{H}_4\text{NMe}_2$ and $\text{Ar}_2 = \text{C}_6\text{F}_5$. This corresponds to a ΔH of -1.84 ± 0.2 kcal/mol and a ΔS of -2.86 ± 0.83 cal/mol·K (Table 2) in favor of the stacking configuration. Hunter and co-workers have reported a study for a pair of arenes with similar structures using their chemical double mutant model system.⁸ Only room temperature study was conducted and a free energy of 0.4 kcal/mol was deduced for the stacking interactions between pentafluoro-aminophenyl and N,N-dimethylaminobenzoate grouping (see below) in CDCl_3 . From our experiments, the ΔH and ΔS in Table 2 give a free energy of 0.99 ± 0.2 kcal/mol at 293 °K in the same solvent.



The difference in the structures between that used in Hunter's experiments and the current experiment may partially account for the difference in observed free energies. The donor and acceptor groups in our model system are more electron-rich and deficient, respectively, than that used in Hunter's experiments. This difference in arene structures may well account for the fact that the attractive interactions in our model system are twice as strong as that determined by the chemical double mutant cycle experiments. Double mutant cycle experiments offer a sophisticated and laborious approach to dissecting a complex system to a single weak interaction. However the method suffers in accuracy as suggested previously,^{10,11} because the flexibility of the system and the uncertainty was multiplied because four different binding studies were required.

The entropies for edge-to-face interactions have been determined by Jennings and coworkers.¹⁴ However, to our knowledge, the entropies for stacking aromatic interactions are for the first time determined experimentally. The entropy values shown in Tables 2–3 are significantly negative when the interactions are strongly attractive. On the other hand, negligible or positive values are obtained when the interactions are small or repulsive. Thus to a certain degree, an enthalpy-entropy compensation is shown in this conformational equilibrium.²⁸ However the entropy decreasing does not completely offset the enthalpy gained through substituent effects. This is evidenced by the different free energies observed for different arene pairs. The errors associated with the entropy values should be greater than the corresponding enthalpy values since the ΔS is derived from the intercept and the ΔH is determined from the slope.

Figure 3 shows a plot of free energy vs. number of fluorine atoms for compounds **6a–6e**, Table 2. The general trend is such that more fluorine substitution leads to higher attractive interaction. This trend follows the reasoning that electrostatic forces dominate the interactions. The quadrupole moments of the fluorinated aromatic rings gradually change from negative to positive as the number of fluorine atoms increases.¹⁷ It follows that attractive interactions occur between the tetra- and penta-fluorinated arene and the $\text{Me}_2\text{NC}_6\text{H}_4$ group while either repulsive interactions occur between the mono-, di-, and tri-fluorinated benzoate and the $\text{Me}_2\text{NC}_6\text{H}_4$ group or the anti conformation becomes attractive in the latter three model compounds. It is interesting to note that although the enthalpies of compounds **6c** ($\text{Ar}_2 = \text{trifluorophenyl}$) and **6d** ($\text{Ar}_2 = \text{difluorophenyl}$) have negative signs, the free energies have positive signs, meaning that entropic effects may play a role for these two compounds.

The trend in Figure 3 is also consistent with a donor-acceptor mechanism, in which the donor is the $\text{C}_6\text{H}_4\text{NMe}_2$ group and the acceptors are fluorinated benzoate groups. As the acceptor

becomes more electron-deficient, the interaction becomes stronger. The pentafluoro substitution has a stronger attractive interaction than the trend line would predict. A UV band at 318 nm was observed for compound **6a**, which was absent in the precursors' spectra. None of the other model compounds showed such UV absorption. We attribute this to charge-transfer interactions. It is consistent with our previous suggestion that in order to observe a charge transfer band in the UV spectrum, a certain threshold of a high HOMO for the donor and low LUMO for the acceptor must be met in order to narrow the energy gap between the donor and the acceptor. When the arene is a relatively weak acceptor,²¹ such as the pentafluorobenzoate group, it appears that the donor must be at least as electron rich as an N,N-dimethylaminophenyl group.

Anti conformation was dominant for all compounds studied where Ar₁ is either a phenyl or a nitrophenyl group except where Ar₂ = C₆F₅ or C₆H₄NO₂ (Table 3). This is in contrast to our recent report on parallel displaced models,¹⁶ where most arenes prefer the syn conformation. The only favorable syn conformation in the current models is when Ar₂ = C₆F₅ or C₆H₄NO₂. Two possible reasons can account for the difference. The first possibility is that sandwich configuration between two aromatic rings are repulsive unless one of the arenes is reasonably electron-deficient. The second possibility is that the imperfect edge-to-face interaction in the anti conformation plays a role in the syn-anti equilibrium. Currently we prefer the first explanation because the highest anti preference (anti/syn = 8.3) is exhibited by model compound **7h** where Ar₁ = C₆H₅ and Ar₂ = C₆H₄CH₃ rather than compound **8g** (anti/syn = 2.3) where Ar₁ = C₆H₄NO₂ and Ar₂ = C₆H₄CH₃. If the edge-to-face interaction in the anti conformation plays a dominant role, one would expect **8g** has a higher anti preference because the nitro group increases the phenyl CH acidity.

A comparison of the observed ratios of *syn* vs. *anti* isomers for the two different model systems is summarized in Table 4. The energy-optimized structures for the two models with C₆F₅ and C₆H₅ are shown in Figure 4 (with triptycene skeleton omitted for clarity). The parallel-displaced model has a smaller interplanar distance. In general, the parallel-displaced models give a greater percentage of *syn* isomers. When one arene is the strongly electron-deficient pentafluorophenyl group, both models prefer the *syn* conformation significantly, but by a comparable margin. The general trend in the attractive stacking interaction towards a pentafluorobenzoate is consistent with a donor-acceptor relationship. For example, the order of preference for the *syn* conformation is Me₂NC₆H₄ > C₆H₅ > O₂NC₆H₄ and in the multi-methyl series the order of preference is Me₃C₆H₂ > Me₂C₆H₃ > MeC₆H₄ > C₆H₅. The observed trend applies when the acceptor is a C₆F₅CO group. When Ar₁ = C₆H₄OMe, the *syn/anti* ratio is smaller than expected. This may be explained by considering the sandwich structure in the *syn* conformation. In the stacked conformation, the oxygen atom of the methoxy substituent is in close proximity to a fluorine atom from the C₆F₅, which causes repulsive interactions. The fact that a charge-transfer band is observed for compound **6a**, where Ar₁ = Me₂NC₆H₄ and Ar₂ = C₆F₅, supports the notion that donor-acceptor interactions play a role.

A much greater difference in *syn/anti* ratio between the two configurations is observed when neither of the arenes is strongly electron-deficient. In these cases, the ratio of the *syn/anti* isomers for the parallel-displaced model is greater than three times of that of the sandwich model. The sandwich model shows a much greater preference for the *anti* isomer indicating either a greater repulsive interaction in the *syn* conformation or a potential attractive interaction in the *anti* conformation although less likely.

Considering the data in whole, we interpret these results by a combination of electrostatic, London dispersive, and charge-transfer effects. When one arene is the strongly electron-deficient pentafluorophenyl group, the dominant role is played by electrostatic (including quadrupolar/dipolar) interactions which exist in both sandwich and the parallel-displaced

configurations. In addition donor-acceptor interactions also play a role as evidenced by the substituent effects and the observation of a charge-transfer band of compound **6a**. The parallel-displaced configuration has the advantage of allowing a closer interplanar distance which enhances London dispersive forces.²¹ This explains why the parallel-displaced configuration in general has a stronger binding energy than the sandwich configuration. When none of the arenes is strongly electron-deficient, electrostatic forces are repulsive in the sandwich configuration while attractive in the parallel-displaced configuration, which explains why the *syn/anti* ratio is three times greater with the parallel-displaced configuration. Thus both electrostatic and dispersive forces favor the parallel-displaced configuration. A further argument for the role of dispersion is to point out that one would mistakenly predict a preferred sandwich conformation for C₆F₆-C₆H₆ interactions if quadrupole moments alone were considered. Recent theoretical studies of C₆F₆-C₆H₆ complex indicate that the parallel-displaced configuration is the energy minimum even for the completely symmetrical aromatic complex.^{21,29}

Summary

Triptycene-derived molecular model system has been used to quantitatively study arene-arene interactions in the near-sandwich configuration. Both enthalpy and entropy are obtained for 21 different compounds via variable temperature NMR spectroscopy. Similar to models with arenes in the parallel-displaced configuration, arene-arene interaction in the sandwich configurations also prefers the *syn* conformation if the two arenes are of opposite polarity, i.e., one electron-rich and the other electron-poor. Overall the sandwich configuration shows a smaller attractive interaction than the parallel-displaced configuration. Electrostatic model based on quadrupole moments alone cannot completely explain the preference for the parallel-displaced arrangement. Our recent theoretical study in conjunction with our previous results has appeared which shows that dispersive forces are important in determining the energy minimum.²¹ The origin of the preference for the parallel-displaced conformation with regard to C₆F₆-C₆H₆ is related to the closeness of stacking.

Experimental Section

Representative procedure for the preparation of the model compounds: 9-(4-Dimethylaminophenoxyethyl)-1-(4-fluorobenzoyloxy)-4-pivaloyloxytriptycene (**6e**)

9-(4-dimethylamino phenoxyethyl)-1-hydroxy-4-pivaloyloxy triptycene (**5**) (0.15 mmol) was treated with 4-fluoro benzoyl chloride (0.19 mmol) and 4-(dimethylamino) pyridine (50 mg, 0.42 mmol) in pyridine (1 ml) at ambient temperature for 24 h. Then 5 ml of 1N HCl was added to quench the reaction. The mixture was extracted with methylene chloride and the extract was washed with aqueous HCl solution two times and dried over MgSO₄. The solvent was removed under reduced pressure. Further purification of the crude via flash column chromatography provided compound **6e** as a solid (96%); M.P. 249–251 °C, ¹H NMR (300 MHz, CDCl₃) δ 7.78–8.36 (2H, m), 7.31–7.42 (5H, m), 6.73–7.03 (7H, m), 6.50–6.52 (4H, m), 5.08–5.62 (3H, m), 2.83 (6H, s), 1.53 (9H, m); ¹³C NMR (75 MHz, CDCl₃) δ 176.4, 164.1, 162.2, 144.3, 143.4, 133.2, 125.7, 125.7, 125.4, 124.6, 123.9, 121.2, 120.3, 116.5, 115.2, 66.3, 55.0, 48.5, 39.4, 32.6, 27.4. HRMS calcd for C₄₁H₃₆FNO₅ + H 642.2656, found 642.2655.

Variable Temperature NMR Experimental Procedure

The ¹H NMR spectra were recorded on a 300 MHz instrument with a variable temperature probe. A 0.05 M solution of the sample in a deuterated solvent such as chloroform was placed in a high quality NMR tube. All samples were degassed using a needle to bubble nitrogen through the sample for ~1 minute. The NMR tube was then capped with a cap and sealed with parafilm. The sample tube was placed into the NMR probe and the air line to the probe was replaced with liquid nitrogen transfer line. The desired temperature was set on the variable

temperature unit and the sample was allowed to equilibrate for 10 ~15 minutes at each set temperature. Then the ^1H NMR spectrum at each temperature was recorded. The ratios of rotamers were obtained through the integrations of selected peaks.

Supplementary Material

Refer to Web version on PubMed Central for supplementary material.

Acknowledgements

Acknowledgment is made to the donors of the Petroleum Research Fund (PRF#40361-AC1) administered by the American Chemical Society. We are grateful for support from the National Institutes of Health (GM069441).

References

1. Kool ET, Morales JC, Guckian KM. Mimicking the structure and function of DNA: Insights into DNA stability and replication. *Angew Chem-Int Edit* 2000;39:990–1009.
2. Coates GW, Dunn AR, Henling LM, Dougherty DA, Grubbs RH. Phenyl-perfluorophenyl stacking interactions: a new strategy for supermolecule construction. *Angewandte Chemie, International Edition in English* 1997;36:248–251.
3. Hunter CA, Lawson KR, Perkins J, Urch CJ. Aromatic interactions. *J Chem Soc-Perkin Trans* 2001;2:651–669.
4. Waters ML. Aromatic interactions in model systems. *Curr Opin Chem Biol* 2002;6:736–741. [PubMed: 12470725]
5. Meyer EA, Castellano RK, Diederich F. Interactions with aromatic rings in chemical and biological recognition. *Angew Chem-Int Edit* 2003;42:1210–1250.
6. Cozzi F, Cinquini M, Annunziata R, Dwyer T, Siegel JS. Polar/Pi Interactions between Stacked Aryls in 1,8-Diarylnaphthalenes. *J Am Chem Soc* 1992;114:5729–5733.
7. Cozzi F, Cinquini M, Annunziata R, Siegel JS. Dominance of Polar/Pi over Charge-Transfer Effects in Stacked Phenyl Interactions. *J Am Chem Soc* 1993;115:5330–5331.
8. Adams H, Blanco JL, Chessari G, Hunter CA, Low CM, Sanderson JM, Vinter JG. Quantitative determination of intermolecular interactions with fluorinated aromatic rings. *Chemistry (Weinheim an der Bergstrasse, Germany)* 2001;7:3494–3503.
9. Cockroft SL, Hunter CA, Lawson KR, Perkins J, Urch CJ. Electrostatic Control of Aromatic Stacking Interactions. *J Am Chem Soc* 2005;127:8594–8595. [PubMed: 15954755]
10. Schneider HJ. Requirements for quantifications of weak intermolecular interactions from equilibrium studies with supramolecular complexes. *Angew Chem-Int Edit Engl* 1997;36:1072–1073.
11. Martinez AG, Barcina JO, Cerezo AD. Influence of highly preorganised 7,7-diphenylnorbornane in the free energy of edge-to-face aromatic interactions. *Chem-Eur J* 2001;7:1171–1175.
12. Paliwal S, Geib S, Wilcox CS. Chemistry of Synthetic Receptors and Functional-Group Arrays. 24. Molecular Torsion Balance for Weak Molecular Recognition Forces - Effects of Tilted-T Edge-to-Face Aromatic Interactions on Conformational Selection and Solid-State Structure. *J Am Chem Soc* 1994;116:4497–4498.
13. Kim E, Paliwal S, Wilcox CS. Measurements of molecular electrostatic field effects in edge- to-face aromatic interactions and CH-pi interactions with implications for protein folding and molecular recognition. *J Am Chem Soc* 1998;120:11192–11193.
14. Jennings WB, Farrell BM, Malone JF. Attractive intramolecular edge-to-face aromatic interactions in flexible organic molecules. *Accounts Chem Res* 2001;34:885–894.
15. Gung BW, Xue XW, Reich HJ. The strength of parallel-displaced arene-arene interactions in chloroform. *J Org Chem* 2005;70:3641–3644. [PubMed: 15845001]
16. Gung BW, Patel M, Xue XW. A threshold for charge transfer in aromatic interactions? A quantitative study of pi-stacking interactions. *J Org Chem* 2005;70:10532–10537. [PubMed: 16323868]
17. Williams JH. The Molecular Electric Quadrupole-Moment and Solid-State Architecture. *Accounts Chem Res* 1993;26:593–598.

18. Luhmer M, Bartik K, Dejaegere A, Bovy P, Reisse J. The Importance Of Quadrupolar Interactions In Molecular Recognition Processes Involving A Phenyl Group. *Bulletin De La Societe Chimique De France* 1994;131:603–606.
19. Cozzi F, Ponzini F, Annunziata R, Cinquini M, Siegel JS. Polar interactions between stacked p systems in fluorinated 1,8-diarylnaphthalenes: importance of quadrupole moments in molecular recognition. *Angewandte Chemie, International Edition in English* 1995;34:1019–1020.
20. Ma JC, Dougherty DA. The cation- π interaction. *Chem Rev* 1997;97:1303–1324. [PubMed: 11851453]
21. Gung BW, Amicangelo JC. Substituent Effects in C₆F₆-C₆H₅X Stacking Interactions. *J Org Chem* 2006;71:9261–9270. [PubMed: 17137351]
22. Sinnokrot MO, Sherrill CD. Substituent effects in π - π interactions: Sandwich and T-shaped configurations. *J Am Chem Soc* 2004;126:7690–7697. [PubMed: 15198617]
23. Tamura Y, Yamamoto G, Oki M. CH₃-O hydrogen bond. Implications of its presence from the substituent effects on the populations of rotamers in 4-substituted 9-ethyl-1-methoxytryptenes and 9-(substituted phenoxyethyl)-1,4-dimethyltryptenes. *Bull Chem Soc Jpn* 1987;60:1781–1788.
24. Kimura N. The Role of the Leaving Group in the Dissociation of Radical Anions of 9-(Aryloxymethyl) anthracenes. *J Am Chem Soc* 2001;123:3824–3825. [PubMed: 11457117]
25. Glaser R. Aspirin. An ab Initio Quantum-Mechanical Study of Conformational Preferences and of Neighboring Group Interactions. *J Org Chem* 2001;66:771–779. [PubMed: 11430095]
26. Gung BW, Xue XW, Reich HJ. Off-center oxygen-arene interactions in solution: A quantitative study. *J Org Chem* 2005;70:7232–7237. [PubMed: 16122242]
27. Shoemaker, DP.; Garland, CW.; Nibler, JW. *Experiments in Physical Chemistry*. 6. McGraw-Hill; New York: 1996.
28. Leffler, JE.; Grunwald, E. *Rates and equilibria of organic reactions as treated by statistical, thermodynamic, and extrathermodynamic methods*. Wiley; New York: 1963.
29. Tsuzuki S, Uchamaru T, Mikami M. Intermolecular interaction between hexafluorobenzene and benzene: Ab initio calculations including CCSD(T) level electron correlation correction. *J Phys Chem A* 2006;110:2027–2033. [PubMed: 16451038]

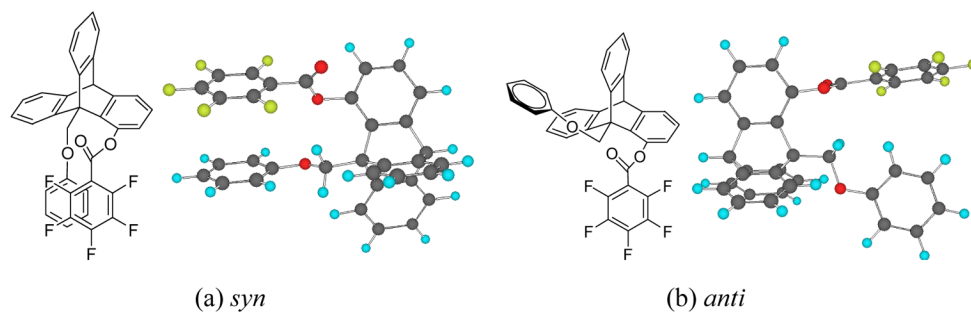


Figure 1. Global ground state conformations for (a) *syn* and (b) *anti* isomers. Ar₁ = phenyl, Ar₂ = pentafluorobenzoate.

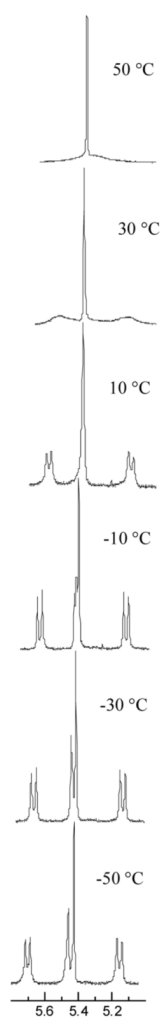
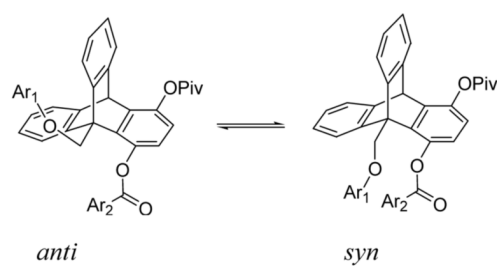


Figure 2. The temperature-dependent NMR signals (300 MHz in CDCl₃) from the bridgehead C(9)H₂ protons of compound **7f**. The sharp singlet is the bridgehead CH at C10.

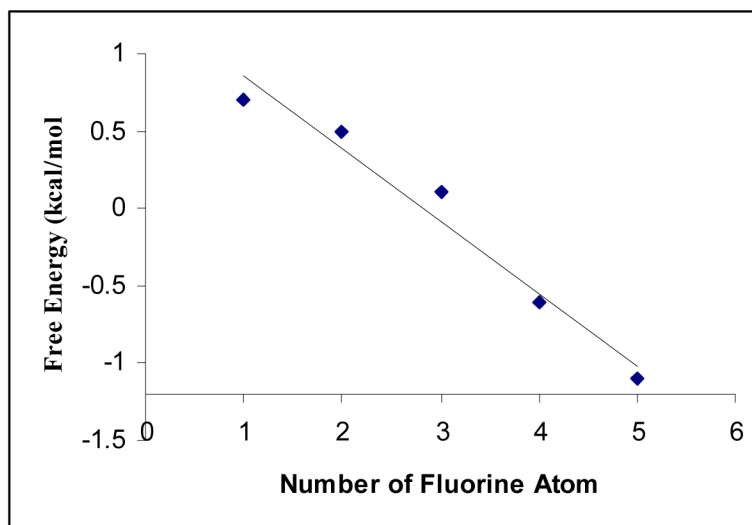


Figure 3. Plot showing the trend in stacking free energy for compounds **6a–6e** as a function of the number of fluorine substitution on Ar_2 ($\text{Ar}_1 = \text{C}_6\text{H}_4\text{NMe}_2$). Primary data are given in Table 1 and Table 2.

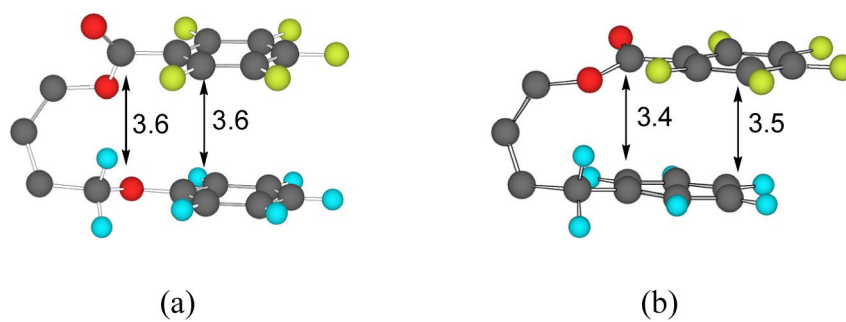
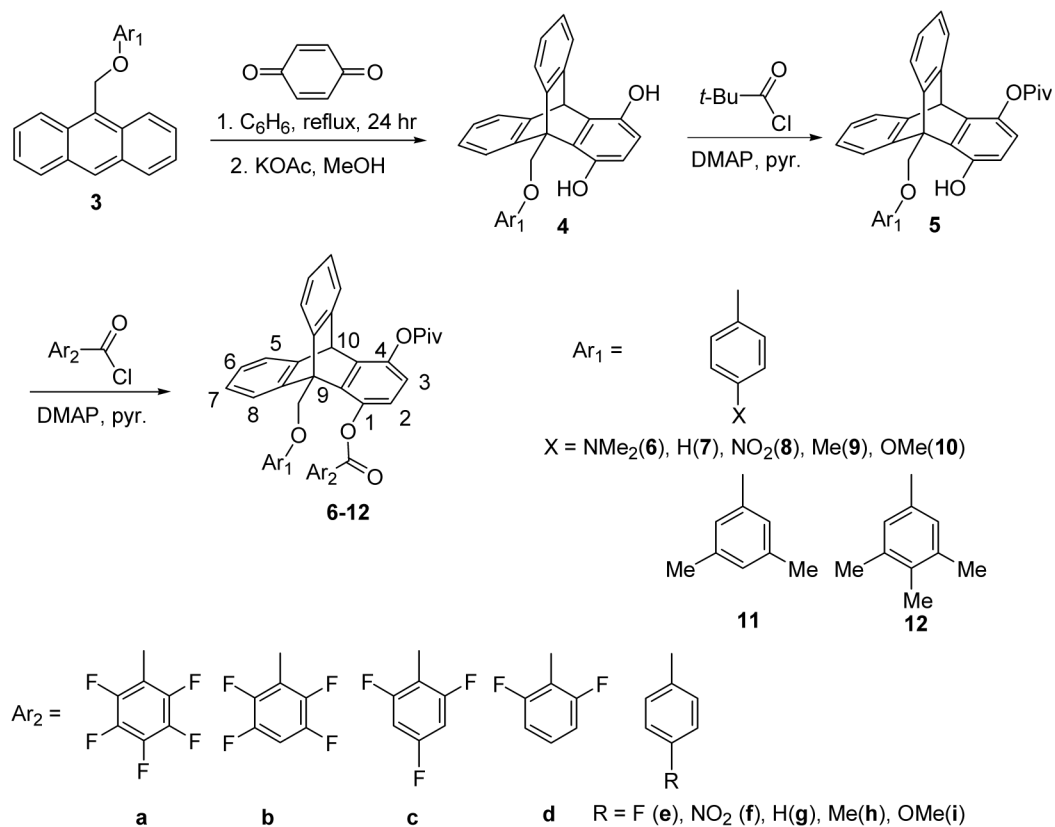


Figure 4. Chem3D representations of (a) sandwich and (b) parallel-displaced models with the triptycene skeleton omitted for clarity. Structures were optimized using MacroModel (version 7.0, force field: MMFFs). Interplanar distances are labeled in angstroms.



Scheme 1.

Ratios of *syn/anti* Isomers at Different Temperatures for Model Compounds **6a-14a**. The experiments were performed in CDCl_3 unless stated otherwise.

Table 1

Entry	Compound	Ar ₁	Ar ₂	<i>syn/anti</i> Ratio in CDCl_3 at different temp.				
				-10	-20	-30	-40	-50 (°C)
1	6a	$\text{C}_6\text{H}_4\text{NMe}_2$	C_6F_5	15.7	17.5	20.7	26.5	28.0
2	6b	$\text{C}_6\text{H}_4\text{NMe}_2$	C_6HF_4	5.37	6.04	6.61	7.36	8.87
3	6c	$\text{C}_6\text{H}_4\text{NMe}_2$	$\text{C}_6\text{H}_2\text{F}_3$	1.62	1.70	1.83	1.90	1.93
4	6d	$\text{C}_6\text{H}_4\text{NMe}_2$	$\text{C}_6\text{H}_3\text{F}_2$	0.72	0.71	0.72	0.72	0.74
5	6e	$\text{C}_6\text{H}_4\text{NMe}_2$	$\text{C}_6\text{H}_4\text{F}$	0.54	0.53	0.48	0.47	0.47
6	7a	C_6H_5	C_6F_5	11.0	11.7	13.7	15.7	18.0
7	7f	C_6H_5	$\text{C}_6\text{H}_4\text{NO}_2$	2.63	2.78	2.94	3.08	3.27
8	7e	C_6H_5	$\text{C}_6\text{H}_4\text{F}$	0.55	0.54	0.53	0.50	0.47
9	7g	C_6H_5	C_6H_5	0.30	0.29	0.26	0.24	0.21
10	7h	C_6H_5	$\text{C}_6\text{H}_4\text{Me}$	0.19	0.17	0.16	0.14	0.12
11	7i	C_6H_5	$\text{C}_6\text{H}_4\text{OMe}$	0.23	0.22	0.19	0.18	0.17
12	8a	$\text{C}_6\text{H}_4\text{NO}_2$	C_6F_5	5.6	6.0	6.8	7.6	8.9
13	8f	$\text{C}_6\text{H}_4\text{NO}_2$	$\text{C}_6\text{H}_4\text{NO}_2$	2.66	2.73	2.85	2.94	3.05
14	8e	$\text{C}_6\text{H}_4\text{NO}_2$	$\text{C}_6\text{H}_4\text{F}$	0.96	0.92	0.90	0.89	0.89
15	8g	$\text{C}_6\text{H}_4\text{NO}_2$	C_6H_5	0.59	0.56	0.55	0.53	0.50
16	8h	$\text{C}_6\text{H}_4\text{NO}_2$	$\text{C}_6\text{H}_4\text{Me}$	0.54	0.51	0.48	0.46	0.44
17	8i	$\text{C}_6\text{H}_4\text{NO}_2$	$\text{C}_6\text{H}_4\text{OMe}$	0.61	0.59	0.57	0.54	0.52
18	9a	$\text{C}_6\text{H}_4\text{Me}$	C_6F_5	13.5	15.2	17.2	18.7	21.3
19	10a	$\text{C}_6\text{H}_4\text{OMe}$	"	10.6	12.0	13.1	15.8	18.2
20	11a	$\text{C}_6\text{H}_3\text{Me}_2$	"	15.2	17.5	19.8	21.0	23.3
21	12a	$\text{C}_6\text{H}_2\text{Me}_3$	"	17.1	19.1	21.3	23.8	26.1
22	13	$\text{C}_6\text{H}_4\text{Me}$	CH_3	1.99	2.08	2.27	2.40	2.58
23	14	CH_3	CH_3	0.32	0.32	0.30	0.28	0.27

The Effect of the Number of Fluorine Atoms of Ar₂ on ΔH and ΔS for Arene-Arene Interactions in CDCl₃. The standard errors are calculated using linear regression analysis.²⁷

Table 2

Entry	Compound	Ar ₁	Ar ₂	$\Delta H^{\circ}_{\text{anti} \rightarrow \text{syn}}{}^a$	$\Delta S^{\circ}_{\text{anti} \rightarrow \text{syn}}{}^b$	$\Delta G^{\circ}_{\text{anti} \rightarrow \text{syn}}{}^c$
1	6a	C ₆ H ₄ NMe ₂	C ₆ F ₅	-1.84 ± 0.2	-2.9 ± 0.8	-0.99 ± 0.2
2	6b	C ₆ H ₄ NMe ₂	C ₆ HF ₄	-1.41 ± 0.1	-3.4 ± 0.3	-0.41 ± 0.1
3	6c	C ₆ H ₄ NMe ₂	C ₆ H ₂ F ₃	-0.53 ± 0.1	-2.4 ± 0.3	-0.17 ± 0.1
4	6d	C ₆ H ₄ NMe ₂	C ₆ H ₂ F ₂	-0.08 ± 0.1	-2.4 ± 0.2	0.62 ± 0.1
5	6e	C ₆ H ₄ NMe ₂	C ₆ H ₄ F	0.46 ± 0.1	-0.9 ± 0.5	0.72 ± 0.1

^a in units of kcal/mol.

^b in units of cal/mol·K.

^c in units of kcal/mol at 293 K.

Table 3
Substituent Effect on the ΔH and ΔS for Arene-Arene Interactions. The standard errors are calculated using linear regression analysis.²⁷

Entry	Compound	Ar ₁	Ar ₂	$\Delta H^{\circ}_{\text{anti-syn}}$ ^a kcal/mol	$\Delta S^{\circ}_{\text{anti-syn}}$ in CDCl ₃ cal/mol·K
1	7a	C ₆ H ₅	C ₆ F ₅	-1.49 ± 0.08	-2.3 ± 0.3
2	7b	C ₆ H ₅	C ₆ H ₄ NO ₂	-0.63 ± 0.02	-1.8 ± 0.1
3	7c	C ₆ H ₅	C ₆ H ₄ F	0.46 ± 0.06	-0.8 ± 0.3
4	7d	C ₆ H ₅	C ₆ H ₅	1.06 ± 0.1	0.3 ± 0.4
5	7e	C ₆ H ₅	C ₆ H ₄ Me	1.30 ± 0.1	0.3 ± 0.4
6	7f	C ₆ H ₅	C ₆ H ₄ OMe	0.93 ± 0.1	-0.8 ± 0.5
7	7g	C ₆ H ₄ NO ₂	C ₆ F ₅	-1.36 ± 0.1	-3.2 ± 0.3
8	7h	C ₆ H ₄ NO ₂	C ₆ H ₄ NO ₂	-0.41 ± 0.1	-1.0 ± 0.1
9	7i	C ₆ H ₄ NO ₂	C ₆ H ₄ F	0.21 ± 0.1	-0.7 ± 0.3
10	7j	C ₆ H ₄ NO ₂	C ₆ H ₅	0.45 ± 0.1	-0.7 ± 0.2
11	7k	C ₆ H ₄ NO ₂	C ₆ H ₄ Me	0.59 ± 0.1	-0.4 ± 0.2
12	7l	C ₆ H ₄ NO ₂	C ₆ H ₄ OMe	0.48 ± 0.1	-0.6 ± 0.1

^aNegative values indicate attractive and positive values repulsive interactions.

Table 4
Comparison between Sandwich and Parallel-displaced π -Stacking

Entry	Compound	Ar ₁	Ar ₂	Ratio (syn/anti, at -15 °C) Sandwich ^a	Parallel-displaced ^b
1	6a	C ₆ H ₄ NMe ₂	C ₆ F ₅	16.6	21.7
2	10a	C ₆ H ₄ OMe	C ₆ F ₅	11.2	16.8
3	7a	C ₆ H ₅	C ₆ F ₅	11.3	13.7
4	7f	C ₆ H ₅	C ₆ H ₄ NO ₂	2.71	9.0
5	7e	C ₆ H ₅	C ₆ H ₄ F	0.55	2.9
6	7g	C ₆ H ₅	C ₆ H ₅	0.30	1.9
7	7i	C ₆ H ₅	C ₆ H ₄ OMe	0.23	1.7

^aThis work.

^bReference 16.